Comparison of CSES ionospheric RO data with COSMIC measurements

Xiuying Wang[1], Wanli Cheng[2], Zihan Zhou[1], Song Xu[1], Dehe Yang[1], Jing Cui[1]

1. Institute of Crustal Dynamics, China Earthquake Administration, Beijing, China
2. Xinyang Station, Henan Earthquake Administration, Henan, China

Corresponding author: Xiuying Wang (652383915@qq.com)

Abstract: CSES (China Seismo-Electromagnetic Satellite) is a newly launched electric-magnetic satellite in China. A GNSS occultation receiver (GOR) is installed on the satellite to retrieve electron density related parameters. In order to validate the radio occultation (RO) data from GOR onboard CSES, a comparison between CSES RO and the co-located COSMIC RO data is conducted to check the consistency and reliability of the CSES RO data using measurements from February 12, 2018 to March 31, 2019. CSES RO peak values (N_mF_2), peak heights (h_mF_2), and electron density profiles (EPDs) are compared with corresponding COSMIC measurements in this study. The results show that: (1) N_mF_2 between CSES and COSMIC is in extremely good agreement with a correlation coefficient of 0.9898. The near zero bias between the two sets is $0.005363\times10^5/cm^3$ with a RMSE of $0.3638\times10^5/cm^3$; and the relative bias is 1.97% with a relative RMSE of 16.17%, which are in accordance with previous studies according to error propagation rules. (2) h_mF_2 between the two missions is also in very good agreement with a correlation coefficient of 0.9385; the mean difference between the two sets is 0.59km with a RMSE of 12.28 km, which is within the error limits of previous studies; (3) Co-located EDPs between the two sets are generally in good agreements, but with a better agreement for data above 200km than that below this altitude. Data at the peak height ranges show the best agreement, and then data above the peak regions; data below the peak regions, especially at the altitude of about the E layer, show relatively large fluctuations. It is concluded that CSES RO data are in good agreement with COSMIC measurements, and the CSES RO data are applicable for most ionospheric-related studies considering the wide acceptance and application of COSMIC RO measurements. However, particular attention should be paid to EDP data below peak regions in application as data at bottom side of the profiles are less reliable than that at the peak and topside regions.

Key words: CSES satellite; COSMIC mission; radio occultation; validation; ionosphere

1. Introduction

The first China Seismo-Electromagnetic Satellite (CSES), also called ZH-1 in China, has been working for over 1 year since its launch on February 2, 2018. This satellite is the first spaced-based geophysical field measurement platform in China, which can be used for the 3-D earthquake observation when combining with the ground-based observation system; a subsequent satellite of this series will be launched in 2022 and the engineering work is under way. The primary scientific objectives of the CSES mission is to obtain world-wide data of space environment of the electromagnetic field, ionospheric plasma and charged particles, to monitor and study the ionospheric perturbations which may possibly associated with earthquake activity, especially with those destructive ones, to support the research on geophysics, space sciences as well as electric wave sciences and so on, and also to provide the data sharing service for international cooperation and scientific community (Shen et al., 2018).

The CSES satellite is sun synchronous orbit with an inclination angle of 97.4°at the altitude of 507 km. The local time of descending and ascending nodes are 1400 and 0200 respectively. It takes about 94.6 minutes to complete a circular orbit, thus about 15 orbits per day. The revisiting period of CSES is 5 days, which means the satellite will nearly repeat the orbits after 5 days. At present, the observation range of the CSES satellite is mainly between -65° and +65°of geographic latitudes (Wang et al., 2019).

There are eight Chinese payloads and one Italian payload onboard the CSES satellite, belonging to 3 categories: (1) electromagnetic observations, including search-coil magnetometer (SCM), electric field detector (EFD), and high precision magnetometer (HPM); (2) ionosphere related observations, including GNSS occultation receiver (GOR), plasma analyzer package (PAP), Langmuir probe (LAP), and tri-band beacon (TBB); (3) and high-energy particles observations, including high energetic particle package (HEPP) and high energetic particle package detector (HEPD), of which HEPD is provided by Italian Space Agency.

Of the eight payloads, four are related to ionospheric parameter observations. The GOR payload onboard CSES is a GPS/BD2 receiver to retrieve ionospheric electron densities according to the radio wave refractivity when traversing the ionosphere. It is known that Low Earth Orbit (LEO) based GPS/GNSS radio occultation (RO) technique has been a powerful technique in ionosphere monitoring; using this technique, the accurate electron density profiles (EDPs) in the ionosphere can be derived with high vertical resolution on a global scale from bending information of the RO signals (Kuo et al., 2004; Rocken et al., 2000; Schreiner et al., 1999). Therefore, many LEO satellites were launched with RO payload after the pioneer RO experiment on GPS/MET mission (Hajj et al., 1998; Schreiner et al., 1999), such as the CHAMP satellite (Jakowski et al., 2002; Wickert et al., 2009), the GRACE satellites (Beyerle et al., 2005), the most famous COSMIC mission (Anthes et al., 2008; Lei et al., 2007), and so on. The application of RO technique is also an important part of the CSES satellite. Combining with the in situ electron density measurements onboard CSES, the CSES RO retrieved electron densities can be used to study global scale ionospheric 3D images from the bottom of the ionosphere to the altitude of the CSES satellite using the large amount of daily occultation events. However, a complete and thorough validation of the RO measurements obtained by the CSES satellite is a necessary work before the retrieved electron density profiles can be used for ionospheric studies.

A primary comparison, between CSES and COSMIC using the global distribution of peak values (N_mF_2) and peak heights (h_mF_2) data, was carried out during the in-orbiting test period of the CSES satellite, and the CSES N_mF_2 values were also compared with the measurements from 3 digisondes in China (Cheng et al., 2018). According to this paper, both the comparisons show that the CSES RO N_mF_2 data are generally consistent with measurements from COSMIC and ionosondes. However, quantitative errors and application suggestions are not given in this paper. Moreover, the comparisons are limited to the peak values and the date coverage is only two months. Therefore, a more complete validation is still required to assess the consistency and reliability of the RO profiles obtained by the CSES satellite. A large amount of RO profiles have been obtained so far by CSES, which provide enough data to implement a more detailed validation work.

Validation of RO profiles is usually done by comparing the profiles with the measurements from ionospheric vertical sounding or incoherent scatter radars (ISRs). However, RO electron density profiles above the F2 peak region cannot be validated by ionosonde observations due to the unreliable extrapolating data at these altitudes. In addition, the uneven distribution of the ionosonde

stations, most located on continental areas and fewer in the ocean areas, restricts the global comparison work. Although ISRs can be used to validate RO electron density profiles above F2 peak region, this comparison is limited due to the relatively small number of ISR sites as well as their limited operating time. Therefore, we will carry out the comparison work using the RO measurements from the COSMIC dataset in this paper.

Validation of the COSMIC electron density measurements has been performed in numerous studies using different measurements, such as the cross validation of the retrieved profiles from nearby spacecraft in the same COSMIC mission (Schreiner et al., 2007), comparison with ground-based ionosondes and ISRs (Cherniak and Zakharenkova, 2014; Chu et al., 2010; Chuo et al., 2011; Habarulema et al., 2014; Kelley et al., 2009; Krankowski et al., 2011; Lei et al., 2007; McNamara and Thompson, 2015), comparison with the in situ electron density measurements (Lai et al., 2013; Pedatella et al., 2015; Yue et al., 2011), comparison with radio tomography data using space climatology phenomenon (Thampi et al., 2011), comparison with ionospheric model IRI (Lei et al., 2007; Wu et al., 2015; Yang et al., 2009), and so on. As COSMIC RO data have been extensively validated and widely accepted for application, COSMIC RO data are used to validate the in situ plasma density observations from the Swarm constellation (Lomidze et al., 2017). We therefore also try to use the COSMIC RO dataset to validate CSES RO measurements because of its relative large amount of data with globally spatial coverage. In addition, similar RO retrieved data from the two sets also provides a unique opportunity to check the consistency and reliability of CSES N_mF_2 and h_mF_2 parameters as well as RO profiles.

In this study, the validation work is implemented by comparing CSES N_mF_2, h_mF_2, and data from EDPs at some selected altitudes with corresponding COSMIC measurements, and the bias and RMSE between the two sets are then calculated and estimated to evaluate the consistency and reliability of CSES RO retrieved data. Based on the results, an application suggestion is given on the CSES ionospheric RO data.

2. Data and Method

2.1 CSES and COSMIC RO data

1. CSES RO data

GOR payload onboard CSES can receive the dual frequencies from GPS (L1: 1575.42MHz±10MHz; L2: 1227.6MHz±10MHz) and DB2 (L1:1561.98MHz±2MHz; L2: 1207.14MHz±2MHz) to retrieve atmospheric and ionospheric parameters with sampling rate of 100Hz and 20Hz respectively. Firstly, TECs from GPS to LEO are calculated from the carrier phase of the dual frequencies; and then electron densities are retrieved from TECs using the Abel integration transformation. The Abel integration method and assumptions used in RO inversion process have been described in detail in many publications (Kuo et al., 2004; Lei et al., 2007; Schreiner et al., 1999) and will therefore not repeat here.

The GOR payload onboard CSES started to work on February 12, 2018 and ionospheric radio occultation (RO) measurements have been conducted since then. CSES RO retrieved data are divided into 5 levels: 0, 1, 2, 2A and 3. Level-0 is original data; Level-1 is physical quantity in time order; Level-2 is physical quantity data with satellite orbital information and geomagnetic

coordinates, while Level-2A is similar with Level 2, but with higher precise orbital information; and Level-3 is 2D structural data product from Level-2 and Level-2A, which can provide peak value, peak height and EDP data.

All the CSES RO data of the 5 levels are saved in HDF5 format, which is organized in a hierarchical way. One file is saved for each occultation event, and about 500 to 600 occultation event files can be obtained per day. Data users can refer to the data specification document for detailed description of data file naming conventions and data level classification, which can be obtained from the CSES data sharing center website www.leos.ac.cn.

More than 180,000 CSES occultation profiles have been obtained from 2018-02-12 to 2019-03-31, of which occultation events co-located with that from the COSMIC mission are used to carry out the comparison and validation work in this paper.

2. COSMIC RO data

The COSMIC (Constellation Observing System for Meteorology, Ionosphere, and Climate, also called FORMOSAT-3 in Taiwan) mission, a constellation of six identical low Earth orbit satellites launched in April 2006, is a joint Taiwan-US mission to observe the near-real-time GPS RO data (Anthes et al., 2008). COSMIC RO data come from the GPS Occultation Experiment (GOX) receivers onboard the COSMIC satellites that monitor the two GPS L-band signals to establish the relative geometries of satellite positions and differences in phase/Doppler shifts (Rocken et al., 2000). At the University Corporation for Atmospheric Research (UCAR) COSMIC Data Analysis and Archive Center (CDAAC), ionospheric profiles are retrieved by use of the Abel inversion technique from TEC along LEO–GPS rays. Detailed description of CDAAC data processing and EDP retrieval method can be found in some literatures (Kuo et al., 2004; Lei et al., 2007).

In the present study, the COSMIC level-2 electron density profiles provided as “ionPrf” files from 2018-02-12 to 2019-03-31 are used, which can be downloaded from CDAAC website https://cdaa-www.cosmic.ucar.edu/. COSMIC can provided over 2000-2500 RO profiles per day at its initial stage, but for now only 200-300 events on average can be obtained each day. Fig.1 gives the total occultation numbers of each month for both CSES and COSMIC missions from February 2018 to March 2019.

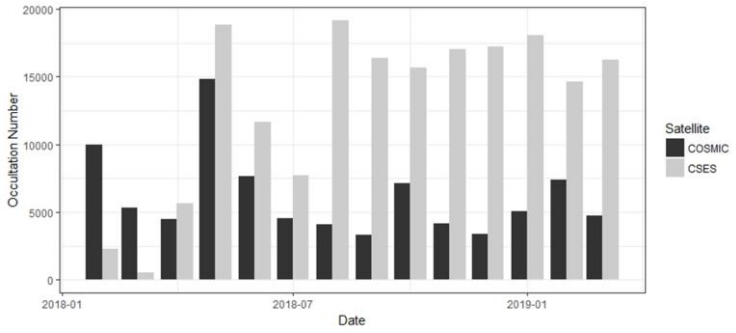

Fig. 1 Occultation number per month from February 2018 to March 2019 for both CSES and COSMIC

From Fig. 1 it can be seen that over 15,000 occultation events can be obtained by CSES each month, or over 500 per day on average, after the initial in-orbit testing stage from February 2018 to July 2018. In contrast, occultation numbers from COSMIC are much less, there are only about 200 occultations on average each day. A total of over 86,000 occultation events have been obtained from the COSMIC data center from February 2018 to March 2019.

Based on these two datasets from CSES and COSMIC, the co-located occultations within defined spatial and temporal criteria from the two measurements are selected and used to carry out

the comparison work.

2.2 Data selection

In order to make the comparison between CSES and COSMIC RO data as accurate as possible, spatial and temporal criteria must be defined to select matching occultation profiles for subsequent comparison analysis.

Before determining the selection criteria, it should be pointed out here that RO retrieved electron density profiles are different from those obtained by vertical ISR observations. For the later, the observation point is fixed, and all the data points of different altitudes on the profiles correspond to this fixed observation point; but for the former, both the LEO and GPS are in motion during the occultation process, therefore data points of different altitudes on the profile correspond to different point on the ground. The geographic location of the tangent points of a RO retrieved profile may vary in several hundred kilometers, which means the spatial range of a profile can cover several degrees in horizontal latitude and longitude range, and several hundred kilometers in vertical altitude range. However, the ionospheric spatial correlation can extent to a large area as suggested by some researches (Shim et al., 2008; Yue et al., 2007). According to Shim et al. (2008), the daytime meridional correlation lengths are approximately 9° and 5° at mid- and low-latitudes, and the nighttime values are about 3° and 2° at mid- and low latitudes, respectively; the zonal correlation lengths are 23° at mid-latitudes and 15° at low latitudes during the day, and are 11° at mid-latitudes and 10° at low latitudes during the night. Therefore, the matching profile pairs from the two missions must be within the correlation distances. Considering the relatively small number of occultation events from the COSMIC measurements, we define the search criteria for co-located occultation events as follows: (1) the time difference between the matching occultation pairs is less than 30 min; (2) the distance differences between the locations of the two occultation events are within 2°×6° range in latitudinal and longitudinal directions. Here, the tangent point at F2 peak value of an occultation profile is defined as the location of the occultation event. The reason to use the peak value tangent point as the occultation location is because the peak value is normally located at the middle of a profile for the CSES EDPs, and by this way the spatial differences of the corresponding points, especially the top and bottom points, between the matching profile pairs can be limited to the correlation distance range as many as possible.

Based on the above criteria, the RO profiles from CSES and COSMIC, covering the period from February 2018 to March 2019, are searched to select the co-located profile pairs. The profiles with N_mF_2 appearing below 200km or above 500 km are discarded, and profiles with only ascending or descending part of a profile which cannot determine the peak values are also deleted from the CSES dataset. A total of 845 matched profiles are found, and their distributions are given in Fig. 2. Numbers of occultation in each 10 latitudinal region are also calculated and given in Fig.3.

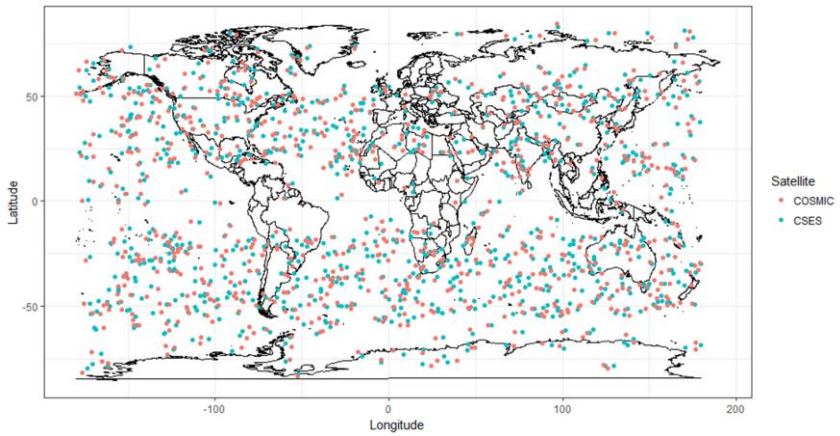

Fig. 2 Distribution of the selected profile pairs

(Each dot indicates the location of the tangent point of the maximum values in a profile.)

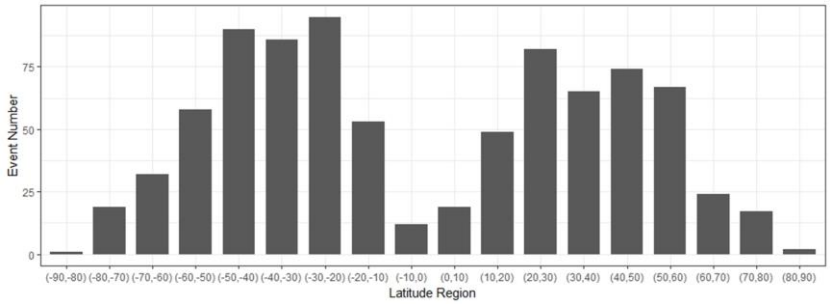

Fig. 3 Number of co-located profile pairs along latitudinal regions

From Fig.2, it can be seen that the selected profile pairs are globally distributed, which makes the data be representative of the whole dataset on spatial scale. In addition, the time coverage of the co-located occultation pairs is over a year, including different periodic components of the ionospheric variations, which makes the data involved in the comparison be representative on temporal scale also.

It is necessary to note that because the CSES satellite is sun-synchronous orbit as mentioned earlier, the local time of the occultation events is concentrated around the ascending (0200) and descending (1400) local time, while COSMIC data cover all the local time. Therefore, special attentions should be paid on the local time issue when combing CSES and COSMIC RO data together for data analysis, that is, occultation events with similar local time as that of CSES must be selected from the COSMIC dataset. This local time issue is not considered by Cheng et al. (2018) when they compared CSES RO data with that from COSMIC, therefore their result is questionable.

Another point to note is that most of the selected profile pairs are distributed in the mid-latitude regions, as shown in Fig. 2 and Fig. 3, and the equatorial region as well as the high latitude regions exhibit lower number of occultation events, which ensures that the selection criteria can be satisfied for most of the selected matched profiles.

2.3 Comparison method

The CSES RO electron density data are compared with the co-located COSMIC RO data to assess the consistency and reliability of the CSES RO data relative to that of the COSMIC, and then the consistency and reliability of the CSES RO data relative to ground-based measurements are

estimated using the results obtained by previous researches on COSMIC RO data according to error propagation rules.

The maximum electron density and its height, namely N_mF_2 and h_mF_2 from CSES RO data, are compared and analyzed directly with the corresponding co-located COSMIC data, respectively. Besides RO peak values, the profiles of the matched pairs are also compared in this study. To compare the similarities of the profiles, average electron density data near some special altitudes of a profile are calculated and compared. Because the orbit altitude of CSES is 507km, only data below this altitude are obtained from the CSES RO retrieved EDPs. Therefore, some altitudes below this altitudes are selected, including 100, 150, 200, 250, 300, 350, 400, 450 and 500 km. It should be pointed out here that selection of these altitudes are of no particular meaning, but for simplification and ease of calculation. The consistency and reliability of the CSES RO profiles are thus evaluated by combining the comparison results of these selected altitudes.

Normally, the height resolution in the F region has the order of 20 km for the COSMIC RO (Kuo et al., 2004), but CSES RO data has a higher resolution due to the higher sampling rate of the radio signals. We therefore use the average data between the selected altitudes±10km, which is just within the vertical resolution of the COSMIC RO data.

In this study, all the selected matched profiles are involved in the analysis rather than those observed in geomagnetic quiet days. In this way, disturbed data caused by events such as geomagnetic storms can also be used to compare their similarities/differences under these special occasions.

3. Results and Discussions

3.1 Comparison of N_mF_2

The maximum electron density in the ionospheric F2 layer, N_mF_2, is the most important parameter in ionospheric related studies. To compare this parameter, the maximum electron density data are extracted from all the matched RO files of CSES and COSMIC measurements. Scatter plot of these matched N_mF_2 points is given in Fig. 4, also given is the histogram of the data differences between the matched peak value points. As shown in Fig. 4b, data differences between the two measurements are normally distributed; points with data differences exceeding 3 times root mean square error (RMSE), shown as open circles in Fig. 4a, are considered outliers and can be eliminated from the selected dataset according to 3σ rule. Red points in Fig. 4a are peak values observed during geomagnetic storm conditions of Dst<-30 nT, all of which are within 3σ limits and matched very well as shown in Fig. 4a. Fig. 4a also gives the linear fitting equation, the goodness-of-fit coefficient R^2 (square of correlation coefficient), and number of data points with elimination of outliers.

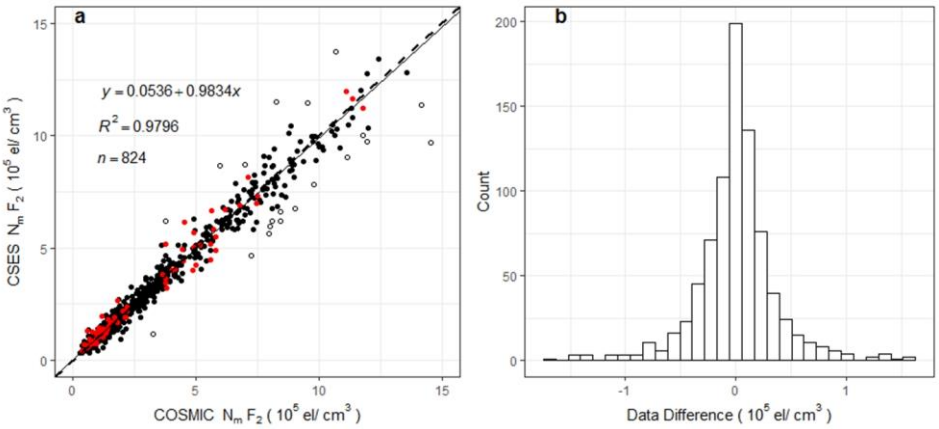

Fig. 4 Scatter plot of matched N_mF_2s and histogram of the data differences between the two sets

(The dash line in Fig. 4a is the equal value line with a slope of 1, and the solid line is the linear fitting line. Open circles are points exceeding 3 times RMSE. Red solid points are data observed when Dst<-30nT. y refers to CSES N_mF_2 data, x COSMIC N_mF_2 data. R^2 is the goodness-of-fit coefficient; n is the total data number after eliminating outliers.)

The correlation coefficient between the two matched N_mF_2 sets with elimination of outliers is 0.9898, and correlation coefficient without elimination of outliers is 0.9795, both of which can pass the significance test of confidence level 0.01. The high correlation coefficient indicates the high consistency between the two N_mF_2 sets. The linear fitting coefficient of 0.9834 given in Fig. 4a is very close to 1; the data differences between the two sets are nearly normal distributed as shown in Fig. 4b, and most of the data differences is around zero, all of which mean that the CSES N_mF_2s are almost equal to COSMIC N_mF_2s with a nearly zero bias. Both the correlation coefficient and the linear fitting coefficient indicate that the CSES N_mF_2s are in extremely good agreement with the corresponding COSMIC data.

To quantify the error, we also calculate the RMSE and relative RMSE between the two sets. The mean of the data differences between CSES N_mF_2 and COSMIC N_mF_2 is $0.005363\times10^5/cm^3$, and the RMSE between the two matched datasets is $0.3638\times10^5/cm^3$, both of which are very small when comparing with the original data. Therefore, the nearly zero bias between the two measurements of N_mF_2 can be neglected, which is in accord with the normal distribution with most data differences clustering around zero as shown in Fig. 4b. The mean relative differences or mean relative deviation (MRD) of N_mF_2 is 1.97%, and the corresponding relative RMSE is 16.17%. The MRD is also extremely small. The mean of data differences and the mean of relative data differences, as well as their RMSEs, again show that the CSES RO data are in very good agreement with the COSMIC data.

To compare the difference of correlation relationship for daytime and nighttime data, the data in Fig. 4 are divided into two groups. As introduced in section 2.2, the local time of CSES satellite is fixed at 0200 during night and 1400 during day, and the local time of RO data are around these two fixed local time, we therefore don't need to further consider differences caused by different local time.

The scatter plots for daytime and nighttime data are drawn using the same method introduced above and given in Fig. 5. The data obtained under geomagnetic storm conditions are also shown in red color, all of which are within the 3σ limits.

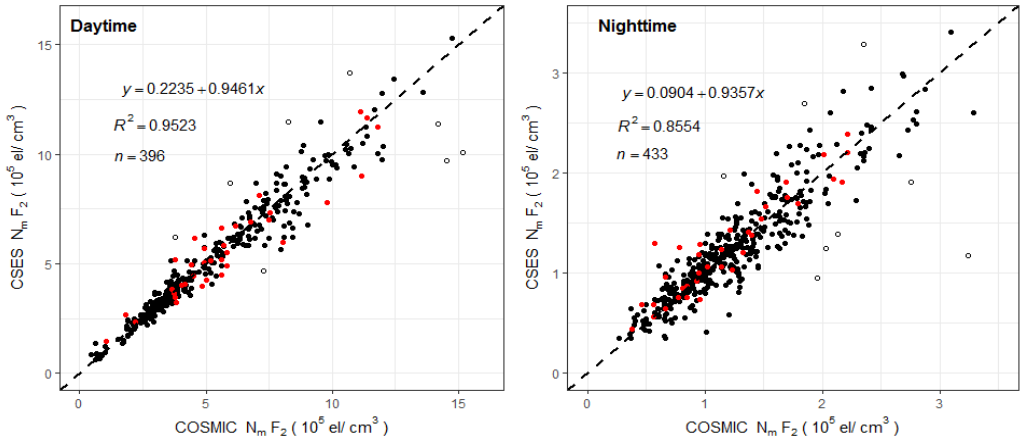

Fig. 5 Scatter plot of N_mF_2 for daytime and nighttime data

(the dash line in Fig. 5 is the equal value line with a slope of 1)

Correlation coefficient for daytime data with elimination of outliers is 0.9759, and 0.9628 without elimination of outliers; for nighttime data with elimination of outliers, correlation coefficient is 0.9249, and 0.8916 for all the data. The higher daytime correlation coefficient indicates a better agreement for the daytime data than the nighttime data. This can be seen clearly from Fig.5, the nighttime data are obviously fluctuated more violently.

The mean data differences for daytime data is -0.04346×10^5 /cm^3 with a RMSE of 0.5865×10^5 /cm^3 , and mean data differences for nighttime data is 0.01215×10^5 /cm^3 with a RMSE of 0.1998×10^5 /cm^3. The opposite sign of the daytime and nighttime mean data differences indicates that the CSES daytime data is slightly smaller than that of the COSMIC, while CSES nighttime data is slightly greater than the corresponding COSMIC data, but both the means of data differences are extremely small and can be consider zero bias when comparing with the original measurements.

Table 1 Absolute and relative error of N_mF_2 between CSES and COSMIC

	Correlation coefficient	Absolute Error		Relative Error	
		Mean (/cm^3)	RMSE (/cm^3)	Mean	RMSE
Total	0.9898	0.005363×10^5	0.3638×10^5	1.97%	16.17%
Daytime	0.9759	-0.04346×10^5	0.5865×10^5	0.79%	12.76%
Nighttime	0.9249	0.01215×10^5	0.1998×10^5	2.61%	18.14%

(Results of all the coefficients and absolute errors maintain 4 significant digits, and relative errors maintain two digits after decimal point. Zeros are padded after the decimal point for some results to maintain an identical power exponent.)

When comparing the different results given in Table 1, the absolute mean data differences for daytime data is obviously greater than that of the overall result, and with an larger RMSE; and the mean data differences for nighttime data is also greater than the overall result, but with a smaller RMSE. It seems that nighttime data are in better agreement than daytime data. However, the two plots in Fig.5 indicate that the daytime data is obvious better than the nighttime data. This is because the daytime data are much greater than nighttime data, absolute error cannot correctly reflect the real situation when comparing data values with different magnitudes. We therefore calculate the relative errors for both the daytime and nighttime data. The mean relative data differences for daytime data is 0.79% with a relative RMSE of 12.76%, and mean relative data difference for nighttime data 2.61% with a relative RMSE of 18.14%, which indicates an obvious better agreement for the daytime measurements.

It is necessary to point out that most of the daytime data points with higher values are located below the dash line as shown in Fig. 5, which means that the COSMIC N_mF_2s are larger than that of the CSES, so there is a negative bias between the two sets; while for nighttime data, most the data points with higher values are above the dash line, indicating greater CSES N_mF_2 values, thus there is a positive bias between them. This can also explain why there is a higher correlation coefficient and a smaller mean data difference when combining daytime and nighttime data together.

Another issue should be pointed out here. As can be seen from Table 1, the absolute mean difference for daytime data is negative, while the mean relative differences is positive. Further analysis shows this different signs is caused by some points with much larger CSES N_mF_2 values.

Here, we compare our results with previous studies and do some analysis.

Lei et al. (2007) obtained a correlation coefficient of 0.85 when comparing COSMIC N_mF_2 with observations from 31 globally distributed SPIDR (The Space Physics Interactive Data Resource, http://spidr.ngdc.noaa.gov/spidr, which is no longer available) ionosondes using data observed in July 2006. Chuo et al. (2013) demonstrated that COSMIC derived N_mF_2 values are in good agreement with digisonde observations of different seasons; they also reported an agreement about 0.96 using observations from a lower latitude ionosonde in souther hemisphere using a big dataset from May 2006 to April 2008. Chu et al. (2010) found a correlation coefficient of 0.98 when comparing N_mF_2s between COSMIC and 60 globally distributed ionosondes belonging to SWPC (Space Weather Prediction Center), NOAA, using data from November 2006 to February 2007. Krankowski et al. (2011) obtained a very good correlation coefficient of 0.986 when validating COSMIC RO data in 2008 using measurements in European mid-latitude ionosondes. Our result of 0.9898 is quite similar to, or even slightly better than those results, when considering the similar solar activity levels. A relative high correlation coefficient between CSES N_mF_2 and ionosondes can be deduced since the correlation transitive conditions are satisfied according to Langford et al. (2001). We therefore obtained that CSES RO derived peak values are in very good agreement with COSMIC and ground-based measurements.

For N_mF_2 relative errors, Krankowski et al. (2011) obtained a mean relative bias of 0.72% with a standard deviation of 8.42%, and the slope of the linear fitting line is 0.994 using a manual selected dataset in Europe, which is better than the results in this paper. Wu et al. (2009) got a -3.2% relative bias with a standard deviation of 20.7% when comparing N_mF_2s between COSMIC and 62 global ionosondes from SPIDR using data from July 2006 to Decemeber 2007. Yue et al. (2011, 2013) suggest that the ability to retrieve N_mF_2 using the Abel inversion technique has an uncertainty about 10%. Based on the linear fitting equation between CSES and COSMIC and on the N_mF_2 relative errors between COSMIC and ground-based measurements, we can deduce that the relative errors between CSES peak values and ground-based measurements are comparable to prior results according to error propagation rules.

As to the absolute error, Kelley et al. (2009) obtained a RMSE of 1.0×10^5 /cm^3 when comparing COSMIC data with ISR; Hajj et al. (2000) obtained a N_mF_2 RMS difference of about 1.5×10^5 /cm^3 when comparing the GPS/MET measurements with nearby ionosonde data, and Jakowski et al. (2002) also obtained a similar RMS difference of about 0.9×10^5 /cm^3 when comparing the CHAMP RO measurements to the in situ Langmuir probe data on the same satellite. Habarulema et al. (2014) suggested that all RO data sets are close to the ionosonde data within similar error margin for both mid-latitude and low-latitude regions when comparing COSMIC, GRACE and CHAMP RO data with that of ionosondes. The absolute errors of our results are much smaller than these results,

indicating an extremely good agreements between CSES and COSMIC RO N_mF_2 and further confirming that CSES RO are also within the general error limit as proposed by Habarulema et al. (2014).

Better result of daytime data in this study is in accord with the conclusion obtained by Wu et al. (2009) and Yue et al. (2011). As we know, the nighttime data has a more complex spatial distribution pattern comparing to daytime data, because daytime data are affected by solar radiation, which makes the global distribution pattern of ionosphere simpler during day time. Larger inversion error will be produced when facing uneven spatial distribution of electron density due to the violence of spherical symmetry assumption of the Abel inversion method. The complex night time spatial distribution can also be proved by the smaller correlation distance during nighttime than that of daytime as discussed in section 3.2 (Shim et al., 2008).

Besides data obtained under geomagnetic quiet days, data obtained under geomagnetic storm conditions are also quite consistent with each other, demonstrating that the RO data between CSES and COSMIC can remain consistency even under disadvantageous conditions. Hu et al. (2014) suggested that COSMIC measurements are acceptable under geomagnetic disturbed conditions when comparing COSMIC RO data with observations obtained from 2008 to 2013 at Sanya, a lower latitude ionosonde in China. We therefore deduce that CSES RO data may be acceptable under geomagnetic disturbed conditions, and we will validate this when enough RO data are accumulated.

As suggested by Schreiner et al. (2007) that co-located RO soundings allow the precision of the technique to be estimated, but not the accuracy. That fact that the nearly zero bias for both daytime and nighttime data and for the overall data, the normal distribution of the data differences, as well as the extremely high correlation coefficient between CSES N_mF_2 and COSMIC N_mF_2, demonstrates that the CSES N_mF_2 data are highly consistent and identical with COSMIC measurements, even under geomagnetic storm conditions, indicating a similar precision of CSES RO N_mF_2 data as that of COSMIC. Given the reliability (accuracy) of the COSMIC data proved by many previous studies, we believe that the CSES N_mF_2 measurements are also quite reliable. Since the co-located data points are globally distributed, the comparison results can be generalized to the overall CSES N_mF_2 dataset obtained so far.

3.2 Comparison of h_mF_2

The height of the maximum peak values in F2 layer, h_mF_2, is also a very important parameter for ionospheric studies. We therefore also compare this parameter using the corresponding COSMIC dataset.

Comparison of the h_mF_2 values between the two sets using the same method as that by N_mF_2, the scatter plot of h_mF_2 and the histogram of the data differences are given in Fig. 6. Data points exceeding 3 times of RMSE, shown as open circles in Fig. 6a, can be deleted from the selected data sets when calculation is implemented. Again, all the peak height points obtained under geomagnetic disturbed condition (red points) are within the 3σ limits as shown in Fig. 6a. It can be seen clearly From Fig. 6a that most of the outliers (open circles) are obviously above the dash line, which means that occasionally RO data from the CSES dataset will much overestimate h_mF_2 values.

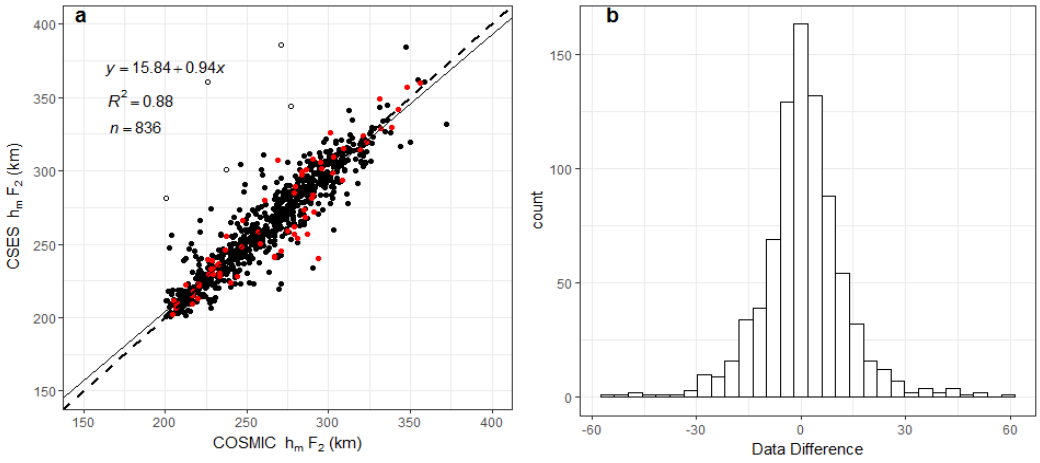

Fig. 6 Scatter plot of h_mF_2s for CSES and COSMIC and histogram of their differences

(The dash line is the equal values line with a slope of 1, and the solid line is the linear fitting line. y refers to the CSES h_mF_2, and x COSMIC h_mF_2. Open circles are points exceeding 3 times standard deviation of data differences between matched points. Red points are peak height obtained under geomagnetic condition of Dst<-30 nT.)

The correlation coefficient of h_mF_2 is 0.9385, though slightly lower than that of the N_mF_2, but can also pass the significance test of confidence level 0.01, which also indicates a very good agreement between the two sets of h_mF_2. The mean of the h_mF_2 data differences (CSES h_mF_2 minus COSMIC h_mF_2) is 0.59 km, which indicates a slight greater h_mF_2 for the CSES peak height values; and the RMSE is 12.28 km. h_mF_2 data difference between the two sets is so small, which can be regarded as nearly zero bias.

Compared with N_mF_2, h_mF_2 data fluctuate more violently. It can be seen from Fig. 6a that some data points are obviously deviated from the data cluster, or from the equal value dash line. Data points above the dash line indicate that CSES h_mF_2s are greater than the corresponding COSMIC data, while data points below the dash line indicate a contrary situation that the COSMIC h_mF_2s are greater than that of CSES. Larger errors are produced by these obviously deviated situations. In spite of the data fluctuation, the nearly zero bias between the two sets, namely the mean data differences, are so small that it can be neglected, which is in accord with the nearly normal distribution of data differences as shown in Fig. 6b. The high correlation coefficient and the normally distributed data differences again indicate that the overall h_mF_2 data of the two sets are in a good agreement.

We also compare the daytime and nighttime h_mF_2s and the corresponding scatter plots are given in Fig. 7. Correlation coefficient for daytime data is 0.9671, and for nighttime 0.8510. Similar as N_mF_2, daytime h_mF_2 has a better correlation coefficient.

The mean data differences for daytime h_mF_2s is 0.40km with a RMSE of 8.59km; while the mean data differences for nighttime h_mF_2s is 0.62km with a RMSE of 14.30km. The positive means of data differences for both daytime and nighttime data indicate that the overall CSES h_mF_2s are slightly greater than that of the COSMIC, but they are so small and can be neglected. The greater RMSE of the nighttime data indicates an obvious more fluctuating nighttime h_mF_2s comparing to the daytime h_mF_2s.

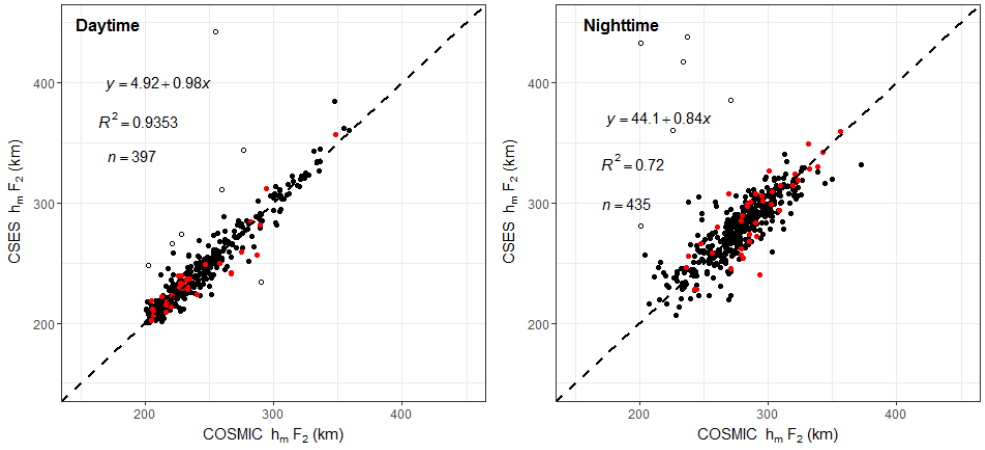

Fig. 7 Scatter plot of h_mF_2 for daytime and nighttime data

(the dash line in Fig. 5 is the equal values line with a slope of 1)

The bias and RMSE for overall, daytime and nighttime data are given in Table 2 for a comparison.

Table 2 Absolute error of h_mF_2 between CSES and COSMIC

	Correlation coefficient	Mean (km)	RMSE (km)
Total	0.9385	0.59	12.28
Daytime	0.9671	0.40	8.59
Nighttime	0.8510	0.62	14.30

From the results shown in Table 2 and Table 1, it can be seen that correlation of N_mF_2 is better than that of h_mF_2 between the two sets. This result is in accord with the conclusion that the RO measurements were better in N_mF_2 than in h_mF_2 (Chuo et al., 2011). Another point is that the daytime h_mF_2s are in better agreement than the nighttime data, which is similar as that of N_mF_2 data.

The overall comparison results of h_mF_2 are very good when comparing to prior COSMIC RO data validation results using ionosondes observations. Chuo et al. (2013) reported an h_mF_2 agreement about 0.87 using observations in low latitude souther hemisphere from May 2006 to April 2008. Krankowski et al. (2011) got a correlation coefficient of 0.949 when comparing COSMIC h_mF_2 data observed in 2008 with that from ionosondes in European mid-latitudes. The high correlation coefficients of our result indicate that the two sets are in good agreement, and the high correlation coefficients between COSMIC h_mF_2 and ionosondes from previous studies can further prove that CSES h_mF_2s are consistent with ionosonde observations based on correlation transitive rule mentioned in Section 3.1.

Krankowski et al. (2011) obtained a bias of 2.8km and a standard deviation of 11.5km when validating the COSMIC h_mF_2 data. Cherniak and Zakharenkova (2014) showed that COSMIC h_mF_2s were in a good agreement with Kharkov ISR observations of different seasons in 2008-2009, and bias and standard deviations are less than 24 km and 29 km respectively. Habarulema et al. (2014) obtained an error limit about 30km when comparing COSMIC h_mF_2s with mid-latitude ionosonde using data in 2008. Yue et al. (2011) suggested that the retrieval uncertainty in h_mF_2 is about 10km for COSMIC simulation analysis. The nearly zero bias and the small RMSE between h_mF_2 of CSES and COSMIC demonstrate that F region peak height parameter obtained by CSES and COSMIC are extremely similar with each other, or in another way, h_mF_2s from the two sets have similar precision and accuracy. We therefore deduce that error between CSES h_mF_2 and ground-based h_mF_2 is comparable to prior results according to error propagation rules.

As a result, the significant correlation coefficient and very small absolute RMSE in this study

indicate the consistent variations and similar precision of h_mF_2 between CSES and COSMIC, and the nearly zero bias indicates the two sets have similar accuracy. All of these results indicate that CSES RO retrieved h_mF_2s are reliable considering the reliability of COSMIC RO data validated by many previous studies.

3.3 Comparison of EDPs

Besides the two most important parameters N_mF_2 and h_mF_2, electron density profiles (EDPs) are also very important because EDPs can provide electron densities at different altitudes to depict ionospheric 3D images from the bottom of ionosphere to the altitude of LEO satellite.

As EDPs from CSES and COSMIC have different altitudes due to the different satellite altitudes of the two missions, only data under the altitude of the CSES satellite can be compared from the co-located profiles. We therefore compare the retrieved EDP data at some selected altitudes as the numbers of data points are not identical for each matched profile pairs, and altitudes of each retrieved data are not identical for the two co-located profile pairs either.

For each altitude specified in section 2.3, we calculate the average data between altitude±10km of each profile and then calculate the correlation coefficients using all the average data pairs at that altitude. The results of all selected altitudes are given in Table 3. Fig.8 gives the scatter plots of all these altitudes, and data obtained in geomagnetic disturbed condition are shown in red points, also shown in the figure are the linear fitting equations, goodness-of-fit coefficients, and numbers of data points involved in the calculation. Outliers are eliminated from the data sets using the same criteria mentioned above.

Table 3 Correlation coefficients and RMSEs for the data at different altitudes of the profiles

Altitude (km)	Correlation Coefficient	Absolute error		Relative error	
		Mean data difference	RMSE	Mean relative data differences	Relative RMSE
500	0.9749	-0.01982×10^5	0.8824×10^5	-1.72%	35.90%
450	0.9882	-0.01551×10^5	0.1070×10^5	-0.69%	27.30%
400	0.9929	-0.01923×10^5	0.1314×10^5	-0.59%	20.29%
350	0.9927	-0.02274×10^5	0.1946×10^5	0.74%	23.45%
300	0.9908	-0.01881×10^5	0.2700×10^5	1.89%	25.16%
250	0.9874	-0.03198×10^5	0.3309×10^5	4.70%	61.29%
200	0.9691	-0.01090×10^5	0.3909×10^5	25.83%	133.77%
150	0.9564	-0.03161×10^5	0.2958×10^5	43.28%	324.74%
100	0.8883	-0.02330×10^5	0.2611×105	78.40%	518.99%

All the correlation coefficients in Table 3 can pass the significance test of confidence level 0.01, which means that data points at different altitudes are highly correlated. When combining all the results together, we can deduce that the co-located profiles from CSES and COSMIC sets are quite similar to each other in spite of the global distribution of these profile pairs as shown in Fig. 2 in Section 2.2. According to some studies, COSMIC profiles are in very good agreement with observations from different ISRs (Lei et al., 2007; Kelley et al., 2009; Cherniak and Zakharenkova, 2014). Pedatella et al. (2015) compared COSMIC RO data at different altitudes with in situ observations from CHAMP and C/NOSF and obtained the correlation coefficients are greater than 0.90, proving the consistency of the COSMIC profiles with in situ satellite observations. Based on

the high consistency between CSES and COSMIC profile pairs and previous COSMIC EDP validation results, we can deduce that CSES profiles may generally agree with ISR profiles according to similarity transitive rules mentioned earlier (Langford et al., 2011), which we will further prove by using ISR observations in our subsequent work.

Schreiner et al. (2007) showed that RMS is about $10^3/cm^3$ between 150 to 500km altitude, whereas below 150km the RMS increases to a maximum of about $3\times10^3/cm^3$ at about 100km, when comparing the RO profiles from different COSMIC satellites within 5km distance. Comparing COSMIC profiles with ISR observations, Lei et al. (2007) suggested inversed errors are larger than $10^5/cm^3$ at altitudes below ~150km and Cherniak and Zakharenkova (2014) obtained an error range of $12\text{-}16\times10^4/cm^3$. Pedatella et al. (2015) obtained an overall bias of $0.22\times10^5/cm^3$ with a standard deviation of $0.65\times10^5/cm^3$, and relative bias and standard deviation are 14.9% and 10.4% respectively, when validating COSMIC data at different altitudes using CHAMP in situ observations; they also compared COSMIC data with C/NOFS in situ observations, and got a relative bias of 5.6% with a standard deviation 12.4%. They attributed the better agreement with in situ observations from C/NOFS to the higher altitude of this satellite. Both the absolute and relative errors, as well as error variation with altitudes shown in Table 3, are in accord with those studies, suggesting that the CSES EDPs are reliable and within general error limits due to the high similarity and consistency between CSES and COSMIC EDPs.

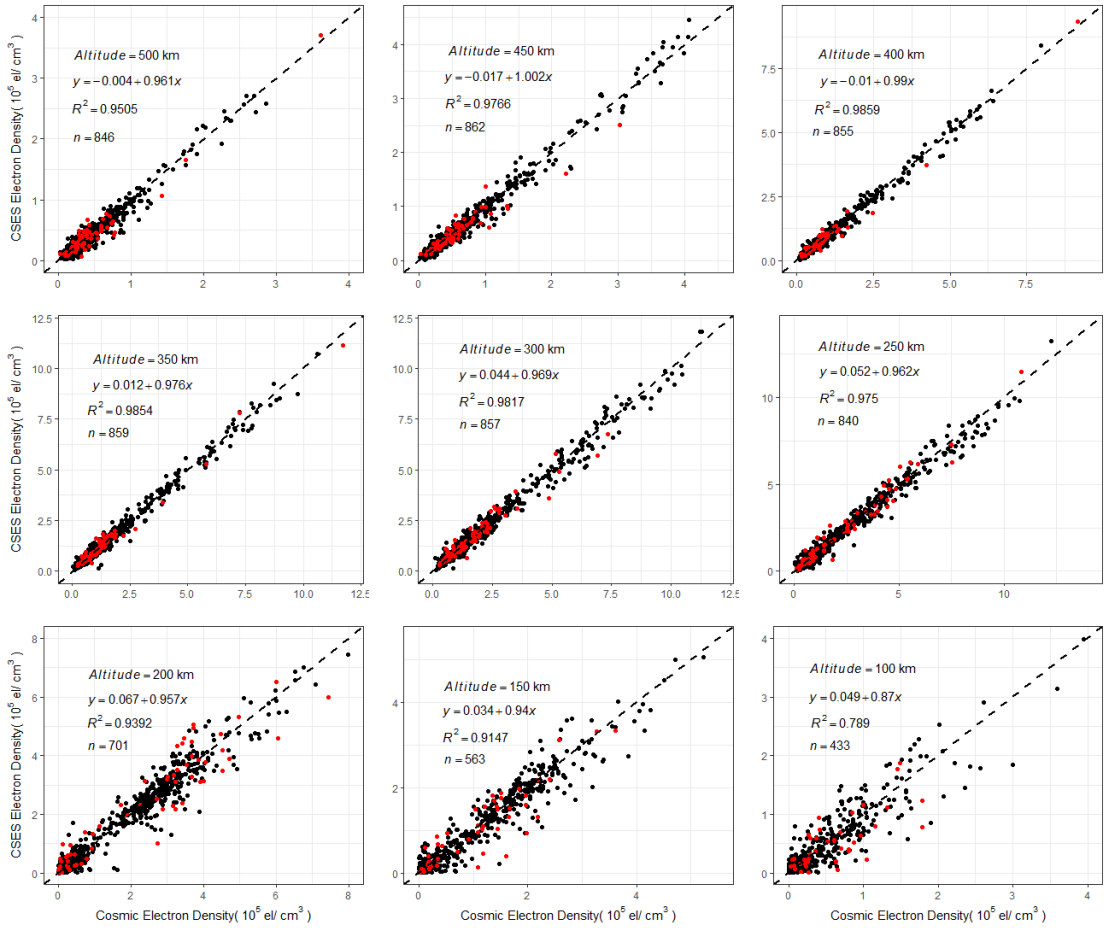

Fig. 8 Scatter plots of data from matched profiles at different altitudes

(the dash line in Fig. 5 is the equal values line with a slope of 1)

From the correlation coefficients given in Table 3, it can be seen that correlation coefficients

above 200 km are obviously greater than those below this altitude. The absolute mean differences at different altitudes are comparable to each other. However, relative differences at different altitudes are quite different; relative mean differences above 200km are extremely small, while relative mean differences below this altitude (include this altitude) increase dramatically. We obtained from Fig. 5 that the peak heights h_mF_2 of most profiles are located between 200km to 350km, the obviously high correlation coefficients in these regions indicate that RO retrieved data at and above peak height are more consistent with each other, whereas discrepancies between the two data sets below the peak regions are much larger. This can be explained by the distribution characteristics of the different ionospheric layers, and by the spherical assumption used in Abel inversion method. As we know, electron density fluctuations in regions above the F2 peak become smaller under geomagnetic quiet condition if comparing with that at lower altitudes due to the relative lower density according to electron density attenuation rules, it is therefore easier to satisfy the spherical symmetry assumption when using the Abel inversion method in this region. This spherical symmetry assumption is by far the most significant error source in the retrieval of the electron density profiles (Lei et al., 2007). In addition, a shorter propagating distance in the topside ionosphere for the radio signals from GPS to LEO will lead to a smaller error of straight line propagation assumption. As suggested by Liu et al. (2010) that COSMIC RO can obtain reasonable correct electron densities around and above F2 peak; however, assumption of spherical symmetry introduces artificial plasma cave and plasma tunnel structures as well as electron density enhancement at the geomagnetic equator at and below 250 km altitude, which will enlarge data discrepancies as shown in Table 3. Syndergaard et al. (2006) also suggested larger errors at the bottom of the retrieved profiles. The results shown in Table 3 in this study are in accord with those studies, demonstrating that CSES EDPs have larger errors for data below 200km altitude, which is similar as that of COSMIC.

An obvious characteristic shown in Table 3 is that all the means of data difference are negative values though they are very small compare to the original measurements, which means the overall CSES data at different altitudes are smaller than the corresponding COSMIC data. The all negative mean data differences at different altitudes may indicate a possible systematic bias between the two measurements. This systematic lower values at all altitudes is most likely caused by the first-order estimation of the electron density at the altitude of the CSES satellite, rather than the spatial differences of the co-located profile pairs, because spatial differences lead to random errors. However, further confirmation of this error sources is required. It is also necessary to point out that the signs of the mean relative data differences at altitudes ≥400km are negative, similar as the signs of the corresponding absolute errors; whereas the signs of the mean relative data differences at altitudes below 400km are positive, just on the contrary to the signs of absolute mean data differences. Further analysis shows that the opposite signs are caused by points where CSES data are much larger than that of COSMIC, and thus lead to extremely larger relative errors, which further indicates that data below the peak regions, especially below about 150km, fluctuate more violently.

Besides spherical symmetry and straight line propagation assumptions, the larger discrepancies at altitudes below peak regions can be explained by the different spatial locations of the matched profiles. Although the peak values of co-located profile pairs are near each other according to selection criteria, data points other than peak values on the matched profile pairs may exceed the selection criteria and result in larger distances due to the different tangent point path of the matched profile pairs. As a result, a larger distance will lead to larger discrepancy between the corresponding data sets. In addition, the tangent point path of the matched profiles may have different directions,

which will lead to different inversion results because each retrieved data represents average electron densities along the radio ray path. In regions with large horizontal gradients, the different ray path can cause obvious difference between the matched profiles. At altitudes below 200km, especially below 150 km, sporadic E-layers can cause large horizontal gradients, and then lead to large inversion error. Wu et al. (2009) suggested that the large relative error below 150 km is due to the errors transferred from upper altitude (the F layer) and the very small electron density at that altitude. They also suggested that the larger ray separations can induce larger errors which can be transferred to low altitudes; phase measurement errors induce small relative fluctuations on the electron density at the topside ionosphere, but can cause large relative fluctuations at low altitude ionosphere, because small electron density at low altitude is sensitive to the phase errors. It is therefore concluded that many sources can cause large errors for measurements at altitudes below 150km, which as a result lead to the large discrepancies between CSES and COSMIC RO data at the bottom of the ionosphere.

Based on the above analysis, we conclude that CSES RO profiles are generally consistent with that of COSMIC very well and are reliable for data applications due to the wide acceptance and application of COSMIC RO data. However, larger discrepancies are found at lower altitudes between the two sets comparing to data differences at higher altitudes. Therefore, special attention should be paid to data below 200km in applications due to the relative large discrepancies between the two datasets.

4. Summary and Conclusions

Validation of the CSES RO data is carried out to estimate the consistency and reliability of the CSES RO data using the globally distributed measurements from the COSMIC mission covering the date range from February 12, 2018 to March 31, 2019 as COSMIC RO data have been widely validated their consistency and reliability using data from different measurements in global scale. Comparing CSES N_mF_2, h_mF_2, and EDP data at some selected altitudes, with corresponding COSMIC RO data, we obtain the following results.

(1) CSES N_mF_2 data are highly consistent with that from COSMIC with a correlation coefficient of 0.9898. The mean data differences is $0.005363\times10^5/cm^3$ with a RMSE of $0.3638\times10^5/cm^3$; the relative mean differences is 1.97% with a relative RMSE of 16.17%. Correlation between daytime N_mF_2 data is obviously better than that of nighttime N_mF_2 data.

(2) CSES h_mF_2 data are also very consistent with COSMIC data, with a correlation coefficient of 0.9385. The bias between the two sets is 0.59km with a RMSE of 12.28km. Again, daytime h_mF_2 has a better correlation than nighttime data.

(3) Co-located profiles between CSES and COSMIC are generally consistent with each other very well, with a better agreement for data at and above peak height regions (200km) than those below this regions. For EDP data below 200km altitude, special attention should be paid due to the relative larger discrepancies between the two sets.

(4) Based on the validation results between COSMIC data and different measurements obtained by many previous studies and the validation results between COSMIC and CSES RO data obtained in this study, it is deduced that CSES RO data are within the error limits obtained by previous studies according to error propagation rules.

GOX payload onboard CSES satellite can obtain over 500 occultation events each day, which

provide a large dataset for the study of 3D distribution of the ionospheric electron density when combining with the in situ electron density measurements obtained by LAP onboard CSES. The relatively thorough comparison work in this paper demonstrates that the CSES RO data are consistent very well with the corresponding COSMIC data, proving that the CSES RO data are reliable for applications on ionospheric-related problems considering the wide applications of the COSMIC RO data. However, as many RO related studies suggest that asymmetry of electron density distribution is the main source of the Abel inversion transformation (Schreiner et al., 1999; Syndergaard et al., 2006; Lei et al., 2007), and this inversion error varies with solar activity, season, geomagnetic latitude and local time (Wu et al., 2009). The CSES RO data in this study cover all the latitudes and four seasons with fixed local time under lower solar activity condition, and solar activity in this study is similar as most of the COSMIC validation studies, the comparison results will therefore applicable to data with similar low solar activity conditions. More subsequent validation work will be conducted and presented using data accumulated under different solar activities.

Data Availability

COSMIC Radio Occultation data used in this paper can be downloaded from https://cdaac-www.cosmic.ucar.edu/ (last access: 22 August, 2019), and CSES Radio Occultation data can be downloaded from www.leos.ac.cn (last access: 27 September, 2019).

Author contribution

Xiuying Wang arranged this study, including: experiment design and data analysis.
Wanli Cheng and Zihan Zhou collected the COSMIC data used in this paper.
Song Xu, Dehe Yang, and Jing Cui did some calculation work to search co-located data.

Competing interests

All authors declare that they have no competing interests.

Acknowledgement

This work is supported by the National Key R&D Program of China under Grant no. 2018YFC1503505, by the Foundation of Institute of Crustal Dynamics, CEA under grant no. ZDJ2018-18 and ZDJ2019-03. COSMIC Radio Occultation data can be downloaded from https://cdaac-www.cosmic.ucar.edu/ (last access: 22 August, 2019). CSES Radio Occultation data can be downloaded from www.leos.ac.cn (last access: 27 September, 2019).

Reference

Anthes, R. A., Bernhardt, P. A., Chen, Y., Cucurull, L., Dymond, K. F., Ector, D., et al.: The COSMIC/FORMOSAT-3 Mission: Early Results, Bulletin of the American Meteorological Society, 89(3), 313–334, doi:10.1175/bams-89-3-313, 2008.

Beyerle, G.: GPS radio occultation with GRACE: Atmospheric profiling utilizing the zero difference technique, Geophysical Research Letters, 32, L13806, doi:10.1029/2005gl023109, 2005.

Cheng Y., Lin J., Shen X. H., Wan X., Li X. X., and Wang W. J.: Analysis of GNSS radio occultation data from satellite ZH-01, Earth and Planetary Physics, 2(6), 499-504, https://doi.org/10.26464/epp2018048, 2018.

Cherniak, I. V., and Zakharenkova, I. E.: Validation of FORMOSAT-3/COSMIC radio occultation electron density profiles by incoherent scatter radar data, Advances in Space Research, 53(9), 1304–1312, doi:10.1016/j.asr.2014.02.010, 2014.

Chu, Y.-H., Su, C.-L., and Ko, H.-T.: A global survey of COSMIC ionospheric peak electron density and its height: A comparison with ground-based ionosonde measurements, Advances in Space Research, 46(4), 431–439, doi:10.1016/j.asr.2009.10.014, 2010.

Chuo, Y.-J., Lee, C.-C., Chen, W.-S., and Reinisch, B. W.: Comparison between bottomside ionospheric profile parameters retrieved from FORMOSAT3 measurements and ground-based observations collected at Jicamarca, Journal of Atmospheric and Solar-Terrestrial Physics, 73(13), 1665–1673, doi:10.1016/j.jastp.2011.02.021, 2011.

Chuo, Y. J., Lee, C. C., Chen, W. S., and Reinisch, B. W.: Comparison of the characteristics of ionospheric parameters obtained from FORMOSAT-3 and digisonde over Ascension Island, Annales Geophysicae, 31(5), 787–794, doi:10.5194/angeo-31-787-2013, 2013.

Habarulema, J. B., Katamzi, Z. T., and Yizengaw, E.: A simultaneous study of ionospheric parameters derived from FORMOSAT-3/COSMIC, GRACE, and CHAMP missions over middle, low, and equatorial latitudes: Comparison with ionosonde data, Journal of Geophysical Research: Space Physics, 119(9), 7732–7744, doi:10.1002/2014ja020192, 2014.

Hajj, G. A., and Romans, L. J.: Ionospheric electron density profiles obtained with the Global Positioning System: Results from the GPS/MET experiment, Radio Science, 33(1), 175–190, doi:10.1029/97rs03183, 1998.

Hu, L., Ning, B., Liu, L., Zhao, B., Chen, Y., and Li, G.: Comparison between ionospheric peak parameters retrieved from COSMIC measurement and ionosonde observation over Sanya, Advances in Space Research, 54(6), 929–938, doi:10.1016/j.asr.2014.05.012, 2014.

Jakowski, N., Wehrenpfennig, A., Heise, S., Reigber, C., Lühr, H., Grunwaldt, L., and Meehan, T. K.: GPS radio occultation measurements of the ionosphere from CHAMP: Early results, Geophysical Research Letters, 29(10), 95-1–95-4, doi:10.1029/2001gl014364, 2002.

Kelley, M. C., Wong, V. K., Aponte, N., Coker, C., Mannucci, A. J., amd Komjathy, A.: Comparison of COSMIC occultation-based electron density profiles and TIP observations with Arecibo incoherent scatter radar data, Radio Science, 44, RS4011, doi:10.1029/2008rs004087, 2009.

Krankowski, A., Zakharenkova, I., Krypiak-Gregorczyk, A., Shagimuratov, I. I., and Wielgosz, P.: Ionospheric electron density observed by FORMOSAT-3/COSMIC over the European region and validated by ionosonde data, Journal of Geodesy, 85(12), 949–964, doi:10.1007/s00190-011-0481-z, 2011.

Kuo, Y.-H., Wee, T.-K., Sokolovskiy, S., Rocken, C., Schreiner, W., Hunt, D., and Anthes, R.: Inversion and Error Estimation of GPS Radio Occultation Data, Journal of the Meteorological Society of Japan, 82(1B), 507–531, doi:10.2151/jmsj.2004.507, 2004.

Lai, P.-C., Burke, W. J., and Gentile, L. C.: Topside electron density profiles observed at low latitudes by COSMIC and compared with in situ ion densities measured by C/NOFS, Journal of Geophysical Research: Space Physics, 118(5), 2670–2680, doi:10.1002/jgra.50287, 2013.

Langford, E., Schwertman, N., and Owens, M.: Is the Property of Being Positively Correlated Transitive? The American Statistician, 55(4), 322–325, doi:10.1198/000313001753272286, 2001.

Lei, J., Syndergaard, S., Burns, A. G., Solomon, S. C., Wang, W., Zeng, Z., et al.: Comparison of COSMIC ionospheric measurements with ground-based observations and model predictions: Preliminary results, Journal of Geophysical Research: Space Physics, 112, A07308, doi:10.1029/2006ja012240, 2007.

Liu, J. Y., Lin, C. Y., Lin, C. H., Tsai, H. F., Solomon, S. C., Sun, Y. Y., et al.: Artificial plasma cave in the low-latitude ionosphere results from the radio occultation inversion of the FORMOSAT-3/COSMIC, Journal of Geophysical Research: Space Physics, 115, A07319, doi:10.1029/2009ja015079, 2010.

Lomidze, L., Knudsen, D. J., Burchill, J., Kouznetsov, A., and Buchert, S. C.: Calibration and Validation of Swarm Plasma Densities

and Electron Temperatures Using Ground-Based Radars and Satellite Radio Occultation Measurements. Radio Science, 53(1), 15–36, doi:10.1002/2017rs006415, 2018.

McNamara, L. F., and Thompson, D. C.: Validation of COSMIC values of foF2 and M(3000)F2 using ground-based ionosondes. Advances in Space Research, 55(1), 163–169, doi:10.1016/j.asr.2014.07.015, 2015.

Pedatella, N. M., Yue, X., and Schreiner, W. S.: Comparison between GPS radio occultation electron densities and in situ satellite observations, Radio Science, 50(6), 518–525, doi:10.1002/2015rs005677, 2015.

Rocken, C., Kuo, Y.-H., Schreiner, W., Hunt, D., Sokolovskiy, S., and McCormick, C.: COSMIC system description, Terr. Atmos. Ocean Sci., 11(1), 21–52, DOI: 10.3319/TAO.2000.11.1.21(COSMIC), 2000.

Schreiner, W., Rocken, C., Sokolovskiy, S., Syndergaard, S., and Hunt, D.: Estimates of the precision of GPS radio occultations from the COSMIC/FORMOSAT-3 mission, Geophysical Research Letters, 34, L04808, doi:10.1029/2006gl027557, 2007.

Schreiner, W. S., Sokolovskiy, S. V., Rocken, C., and Hunt, D. C.: Analysis and validation of GPS/MET radio occultation data in the ionosphere, Radio Science, 34(4), 949–966, doi:10.1029/1999rs900034, 1999.

Shen, X., Zhang, X., Yuan, S., Wang, L., Cao, J., Huang, J., et al.: The state-of-the-art of the China Seismo-Electromagnetic Satellite mission, Science China Technological Sciences, 61(5), 634–642, doi:10.1007/s11431-018-9242-0, 2018.

Shim, J. S., Scherliess, L., Schunk, R. W., and Thompson, D. C.: Spatial correlations of day-to-day ionospheric total electron content variability obtained from ground-based GPS, Journal of Geophysical Research: Space Physics, 113, A09309, doi:10.1029/2007ja012635, 2008.

Syndergaard, S., W. S. Schreiner, C. Rocken, D. C. Hunt, and K. F. Dymond: Preparing for COSMIC: Inversion and analysis of ionospheric data products, in Atmosphere and Climate: Studies by Occultation Methods, edited by U. Foelsche, G. Kirchengast, and A. K. Steiner, pp. 137–146, Springer, New York, 2006.

Thampi, S. V., Yamamoto, M., Lin, C., and Liu, H.: Comparison of FORMOSAT-3/COSMIC radio occultation measurements with radio tomography, Radio Science, 46, RS3001, doi:10.1029/2010rs004431, 2011.

Wang, X., Cheng, W., Yang, D., and Liu, D. Preliminary validation of in situ electron density measurements onboard CSES using observations from Swarm Satellites, Advances in Space Research, doi:10.1016/j.asr.2019.05.025, 2019.

Wickert, J., Michalak, G., Schmidt, T., Beyerle, G., Cheng, C.-Z., Healy, S. B.: GPS Radio Occultation: Results from CHAMP, GRACE and FORMOSAT-3/COSMIC, Terrestrial, Atmospheric and Oceanic Sciences, 20(1), 35-50, doi:10.3319/tao.2007.12.26.01(f3c), 2009.

Wu, X., Hu, X., Gong, X., Zhang, X., and Wang, X.: Analysis of inversion errors of ionospheric radio occultation, GPS Solutions, 13(3), 231–239, doi:10.1007/s10291-008-0116-x, 2009.

Wu, K.-H., Su, C.-L., and Chu, Y.-H.: Improvement of GPS radio occultation retrieval error of E region electron density: COSMIC measurement and IRI model simulation, Journal of Geophysical Research: Space Physics, 120(3), 2299–2315, doi:10.1002/2014ja020622, 2015.

Yang, K.-F., Chu, Y.-H., Su, C.-L., Ko, H.-T., and Wang, C.-Y.: An Examination of FORMOSAT-3/COSMIC Ionospheric Electron Density Profile: Data Quality Criteria and Comparisons with the IRI Model, Terrestrial, Atmospheric and Oceanic Sciences, 20(1), 193-206, doi:10.3319/tao.2007.10.05.01(f3c), 2009.

Yue, X., Schreiner, W. S., Kuo, Y.-H., Wu, Q., Deng, Y., and Wang, W.: GNSS radio occultation (RO) derived electron density quality in high latitude and polar region: NCAR-TIEGCM simulation and real data evaluation, Journal of Atmospheric and Solar-Terrestrial Physics, 98, 39–49, doi:10.1016/j.jastp.2013.03.009, 2013.

Yue, X., Schreiner, W. S., Rocken, C., and Kuo, Y.-H.: Evaluation of the orbit altitude electron density estimation and its effect on the Abel inversion from radio occultation measurements, Radio Science, 46, RS1013, doi:10.1029/2010rs004514, 2011.

Yue, X., Wan, W., Liu, L., and Mao, T.: Statistical analysis on spatial correlation of ionospheric day-to-day variability by using GPS and Incoherent Scatter Radar observations, Annales Geophysicae, 25(8), 1815–1825, doi:10.5194/angeo-25-1815-2007, 2007.